Extreme-ultraviolet radiation filtering by freestanding transmission gratings

Mike Gruntman

Measurement of energetic neutral atoms fluxes in space requires efficient suppression of exceptionally strong background extreme-ultraviolet (EUV) and UV radiation. Diffraction filters make it possible to separate (transmit) charged and neutral particles from the background radiation (which would be suppressed). Recently developed freestanding transmission gratings look especially promising for implementation in a new family of diffraction EUV/UV filters. The first results of our experimental study of filtering properties of freestanding transmission gratings with a period of 200 nm are presented. The grating transmission was measured in the 52–131-nm wavelength range, and grating polarization properties were determined at 58.4 nm. It is shown that transmission gratings can be used efficiently as filters and polarizers in the EUV/UV spectral range.

Key words: Transmission grating, polarization, EUV filters, diffraction filters.

1. Introduction

Filtering the radiation in the extreme-ultraviolet (EUV) spectral range is required in many space and laboratory applications. I report here first results of my experimental study of the filtering properties of freestanding transmission gratings in the 50–131-nm wavelength range. A freestanding transmission grating consists of a set of parallel gold bars separated by gaps and supported by an additional large-mesh grid. A filter based on freestanding transmission gratings would make it possible to separate (transmit) charged and neutral particles from the background EUV/UV radiation (which would be suppressed). Unique properties of such filters permit substantial improvement in the performance of instruments for detection of energetic neutral atom (ENA) fluxes in space plasmas.[1] Imaging of the heliosphere and planetary magnetospheres in ENA fluxes is recognized as a powerful tool in the study of global processes in space.[2,3] ENA instruments, which have been developed gradually over the last 25 years, are rapidly maturing in preparation for forthcoming space missions, such as that of the Cassini and Magnetosphere Imager.

ENA detection in space is notoriously difficult[2,4] because of the extremely low intensity of neutral atom fluxes and because of ENA instrument exposure to a high level of background EUV/UV radiation ($\lambda < 150$ nm). In the case of Earth the brightest background lines belong to emissions of hydrogen, helium, oxygen, and nitrogen atoms, molecules and ions in the 30–140-nm range,[5] the dayglow brightness being $\sim$10 kR (1 R = 1 Rayleigh = $10^6/4\pi$ photon cm^{-2} s^{-1} sr^{-1}). In the heliosphere the background radiation is concentrated in the hydrogen Lyman-α resonance line (121.6 nm) and in the helium resonance line (58.4 nm). The heliospheric background radiation is anisotropic, and its brightness varies in the inner heliosphere between 300 and 1000 R for the hydrogen line and between 1 and 10 R for the helium line.

Currently available techniques to suppress the background EUV/UV radiation limit ENA instrument capabilities and distort ENA characteristics.[2,4] As first suggested more than a decade ago,[6] diffraction filters can provide efficient suppression of the EUV radiation and high transparency to ENA's. Diffraction filtering is based on the fact that photons can easily pass through a straight channel-pore (slit) in a filter if the channel diameter (slit width) is much larger than the photon wavelength. In contrast to photons an ENA passes through the channel freely if it does not collide with the channel walls. Thus diffraction filters permit the separation of incident ENA's from EUV/UV photons and would serve as particle collimators.[1] The requirements for filters

The author is with the Department of Aerospace Engineering, MC-1191, University of Southern California, Los Angeles, California 90089-1191.

Received 9 January 1995; revised manuscript received 17 March 1995.

0003-6935/95/255732-06$06.00/0.

(to be used in space experiments) include efficient suppression of EUV/UV radiation, high transparency to ENA's (i.e., high geometrical transparency), and mechanical robustness to withstand the vibrations and shocks of rocket launch. Diffraction filters can be used for suppression of the background EUV/UV radiation in fusion plasma diagnostics as well.

Radiation suppression in the EUV/UV spectral range requires diffraction filters with an opening size of 100 nm or less. Early research to evaluate submicrometer structures with the desired properties was started by Gruntman and Leonas[6] for ENA imaging and simultaneously and independently by Mitrofanov[7] for EUV astronomical applications. This early research was based on the so-called nuclear track filters (NTF's) (see Ref. 1). The technology of NTF fabrication as well as the application of various NTF's are described in detail elsewhere.[8–10] Although the EUV/UV filtering by NTF's has been successfully demonstrated,[7,11] NTF's are of limited practical use for ENA imaging because of their inherently low geometrical transparency.[1] A review[1] of several possible alternative technologies pointed to promising characteristics of freestanding transmission gratings that should both attenuate and polarize radiation.

A schematic view of a freestanding transmission grating is shown in Fig. 1. The grating consists of a set of parallel gold bars with a period p and a geometrical transparency, $g = d/p$, of approximately one half. The grating bars are supported by an additional large-mesh grid (not shown in the figure) that makes an overall grating geometrical transparency of ≈ 0.25. Gratings are manufactured at the Massachusetts Institute of Technology by a sequence of technological steps including holographic lithography, ion and reactive-ion etching, and electroplating.[12,13] The gratings are being developed for NASA's Advanced X-Ray Astrophysics Facility (AXAF) where 336 transmission gratings will be flown as a part of the High Energy Transmission Grating Spectrometer. Although the AXAF requirements are confined to thin-film-supported gratings, a spin-off of the new technology are freestanding transmission gratings. Freestanding transmission gratings are designed to withstand the mechanical requirements of space flight and will be flown for the first time on the Solar Heliospheric Observatory mission.[14]

Transmission gratings, which can be used in standalone or crossed tandem configurations,[1] would permit one to achieve efficient EUV/UV radiation suppression and high (5–25%) geometrical transparency, the latter feature being indispensable for ENA space experiments. Data on EUV radiation transmission through submicrometer openings are scarce; the experimental study of transmission grating characteristics in the EUV spectral range was started only recently.[15–17] I report here first experimental results from my study of the transmission and polarization properties of gold transmission gratings with a period of $p = 200$ nm in the 52–131-nm-wavelength range.

2. Experiment

A schematic of the experiment is shown in Fig. 2. Monochromatic EUV radiation was produced by a dc glow-discharge source followed by a 0.5-m Seya–Namioka EUV monochromator. The transmission of a single grating was measured in the 52–131-nm-wavelength range, and grating polarization properties were determined at 58.4 nm. The nominal geometrical characteristics of gratings, as provided by the manufacturer, were the following: period, $p = 200$ nm; distance between the metal bars, $d = 100$ nm (i.e., geometrical transparency, $g = 0.5$); length, $h = 435$ nm (Fig. 1); grating area, 5×11 mm. The grating serves as a particle $\pm 6.6°$ collimator in one dimension. The geometrical transparency of a large-mesh grid supporting the grating was 0.48. This type of gold grating is commercially available from X-Opt Inc., Gainesville, Fla. 32605. The characterization of fabricated transmission gratings is a nontrivial task, and possible deviations from nominal geometrical characteristics are discussed below.

Grating filtering and polarization properties are interdependent because the grating transmission strongly depends on the incident light polarization. This polarization dependence significantly complicates the experimental study of grating properties that requires accurate knowledge of the photon-beam polarization. The light produced by a glow-discharge source is unpolarized, but it becomes partially polarized after reflecting from the diffraction (reflection) grating in the Seya–Namioka monochromator. A gold diffraction (reflection) grating with 1200

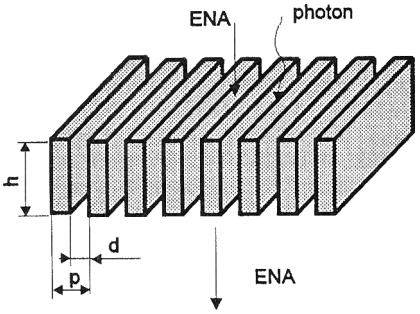

Fig. 1. Schematic view of a freestanding transmission grating. (The supporting large-mesh grid is not shown.)

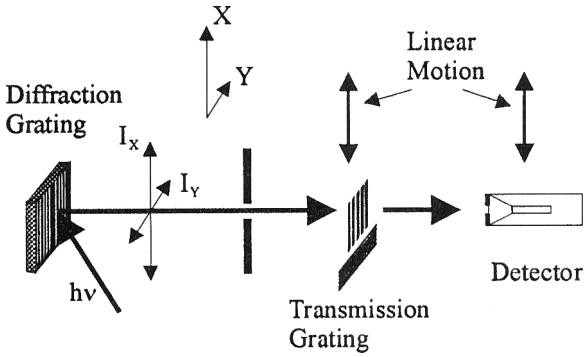

Fig. 2. Measurement scheme for studying the transmission and polarization properties of transmission gratings.

lines/mm and blazed at 70 nm was used in the monochromator.

The polarization of the light exiting the monochromator (which is used to study transmission gratings) is unknown. It is assumed that the light beam consists of two linearly polarized components (along mutually perpendicular X and Y axes) with intensities I_X and I_Y; the total photon-beam intensity is $I_0 = I_X + I_Y$ (Fig. 2). The X axis is parallel to the grooves of the diffraction grating in the monochromator (i.e., normal to the plane of incidence), and the Y axis is parallel to the incidence plane; the X and Y axes are perpendicular to the photon-beam direction. Polarization P_0 of the light exiting the monochromator is given by

$$P_0 = (I_X - I_Y)/(I_X + I_Y). \tag{1}$$

A transmission grating, mounted normal to the photon beam, can be moved in and out of the beam by a linear motion mechanism (Fig. 2). A photon detector (channel electron multiplier) can also be moved in a direction perpendicular to the beam axis. The alignment of both the grating and the detector in the Y-axis direction was achieved by additional rotary motion. This experimental arrangement permitted us to measure the transmission of the transmission gratings as well as to monitor the background count rate. It was verified by detector scanning that the zeroth-diffraction-order beam was always measured after the grating. The photon beam was collimated by several slits, and the detector aperture was selected in such a way as to intercept all transmitted photons in the zeroth diffraction order. The channel electron amplifier was in a linear counting mode; no attempt to account for (possibly small) detection efficiency dependence on light polarization[18] has been made. Only reliably identified spectral lines were used for transmission measurements in the range from 52.2 to 130.4 nm; helium was used as a working gas in the dc glow-discharge light source.

The following measurements were performed:

(1) Single-grating transmission for two orthogonal grating orientations, one with the grating metal bars parallel to the reflection grating in the monochromator (i.e., parallel to the X axis) and another for the perpendicular orientation (i.e., parallel to the Y axis).

(2) Transmission of two crossed gratings (i.e., two gratings normal to the beam and installed in series, or tandem, with perpendicularly oriented metal bars).

3. Model

Let the grating transmission T_P be the transmission of the light polarized parallel to the transmission grating metal bars and the grating transmission T_S be the transmission of the light polarized perpendicular to the grating metal bars. It is assumed that the incident light beam, which is linearly polarized parallel (perpendicular) to the grating bars, is attenuated without the production of a component perpendicular (parallel) to the grating bars after the grating.

The following intensities (detector count rates) are measured: the intensity of the unobstructed photon beam (count rate C_0) and the intensity of the attenuated beam (zeroth diffraction order) with two grating orientations, namely, grating bars parallel to the X axis (count rate C_X) and Y axis (C_Y), respectively. It is convenient for one to present measurement results using normalized count rates, $R_X = C_X/C_0$ and $R_Y = C_Y/C_0$, which permits one to eliminate the unknown photon detection efficiency of the detector. The normalized count rates can be related to the grating transmissions, $T_P(\lambda)$ and $T_S(\lambda)$, as

$$R_X(\lambda) = [I_X(\lambda)T_P(\lambda) + I_Y(\lambda)T_S(\lambda)]/I_0(\lambda), \tag{2}$$

$$R_Y(\lambda) = [I_X(\lambda)T_S(\lambda) + I_Y(\lambda)T_P(\lambda)]/I_0(\lambda). \tag{3}$$

By adding and subtracting Eqs. (2) and (3), one obtains the sum T_Σ of single-grating transmissions,

$$T_\Sigma(\lambda) = T_P(\lambda) + T_S(\lambda) = R_X(\lambda) + R_Y(\lambda), \tag{4}$$

and the polarization of the incident light, i.e., the light exiting the monochromator,

$$P(\lambda) = [R_X(\lambda) - R_Y(\lambda)]/[T_P(\lambda) - T_S(\lambda)]. \tag{5}$$

The transmission T_X of the crossed grating configuration would be

$$T_X = T_P \times T_S, \tag{6}$$

and it is independent of the incident light polarization. Thus, by experimentally determining the sum of single-grating transmissions, T_Σ (by measuring R_X and R_Y) and measuring the transmission T_X of crossed gratings, one unambiguously obtains grating transmissions T_P and T_S. Knowledge of the transmissions, $T_P(\lambda)$ and $T_S(\lambda)$, permits the determination of radiation filtering (suppression) properties of various grating configurations.

Filtering unpolarized light by a single transmission grating is important for the applications case. A single transmission grating would attenuate the light and serve as a polarizer. The transmission of the incident unpolarized light T_0 by a single grating would be

$$T_0 = (T_P + T_S)/2 = T_\Sigma/2, \tag{7}$$

and the polarization P_T of the transmitted light would be

$$P_T = (T_P - T_S)/(T_P + T_S). \tag{8}$$

The transmitted light would be highly polarized if $T_P \gg T_S$; in such a case a transmission grating serves as an efficient polarizer. The suppression of unpolarized light by a single grating depends on the transmission $(T_P + T_S) = T_\Sigma$ only, and the determination of T_Σ does not require measurements with crossed gratings.

An adequate theoretical model of the radiation transmission through gratings is highly desirable for

predicting grating filtering properties without expensive trial-and-error fabrication. The only comprehensive theoretical model and the computer code simulating transmission-grating optical properties known to the author were developed by Anderson.[19] The discussion of the model and computer code is beyond the scope of this paper and can be found elsewhere.[16,18] We compare computer-code predictions with our measurement results because experimental verification of Anderson's model and code is an important task.

The complex dielectric constants, $\epsilon = \epsilon_1 - i\epsilon_2$, of the grating material (gold) are used as input parameters for the computer code.[19] The dielectric constants are related to the index of refraction n and the extinction coefficient k through the following equations: $\epsilon_1 = n^2 - k^2$ and $\epsilon_2 = 2nk$. The optical characteristics of gold in the EUV spectral range are known with some uncertainty, and they may depend on fabrication specifics and surface-preparation techniques. We used in our computer simulations two sets of gold optical constants, those from Weaver *et al.*[20] and those from Lynch and Hunter.[21] These optical constant sets are referred to as the WKLK and LH sets, respectively.

Figure 3 shows the spectral dependence of optical constants n and k for the WKLK and LH sets. The optical constants are given only at points where experimental measurements were performed. All points are connected by straight lines to guide the eye. We also extended computer simulation beyond the experimentally studied spectral range down to 30.4 nm to include this line, which is important for space applications.

One can clearly see that two optical constant sets are compatible for short wavelengths, $\lambda < 60$ nm, but show a substantial discrepancy for longer wavelengths. Computer simulations performed for both optical constant sets showed that the transmission T_S is especially sensitive (to as high as a factor of 40) to the uncertainty in optical constants for $\lambda > 80$ nm, although transmission T_P varies only slightly (by a factor of 2). Because $T_P \gg T_S$ for $\lambda > 80$ nm (see below), transmission T_Σ and consequently predictions of the transmission of unpolarized light by a single grating would thus be only slightly sensitive to the uncertainty in optical constants. The difference between the values of T_Σ computed for the LH and WKLK gold constant sets gradually increases with the wavelength increase, and it does not exceed a factor of 2.

The transmission of unpolarized light by crossed gratings, which is determined by a product of T_P and T_S, strongly depends on optical constants. The difference between the computed values of the transmission T_X for two optical constant sets is small at short wavelengths and increases significantly for longer wavelengths.

4. Results and Discussion

The sum of the single-grating transmissions, $T_\Sigma = T_P + T_S$, was experimentally obtained at 12 wavelengths in the range from 52.2 to 130.4 nm. The transmission T_X by crossed gratings was measured at the 58.4-nm wavelength only. The measured dependence $T_\Sigma(\lambda)$ is compared with the computer simulation results in Fig. 4; computations are presented here for the LH optical constant set only. The measurement accuracy is better than $\pm 5\%$, and it is determined by the counting statistics and experimentally monitored stability of the light beam. Here and below, all experimental points as well as calculated points are connected by straight lines to guide the eye.

The computed spectral dependence of the grating transmission, which uses nominal grating geometrical parameters ($g = 0.5$), differs substantially from measurement results (Fig. 4). Experimentally determined values of $T_\Sigma(\lambda)$ are not only much lower, for example, by a factor of 30 at 121.6 nm, but also the spectral dependence of the transmission is different.

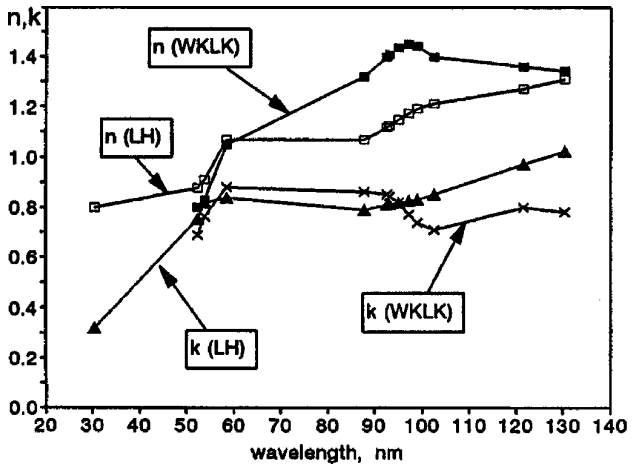

Fig. 3. Spectral dependence of index of refraction n and extinction coefficient k for gold.

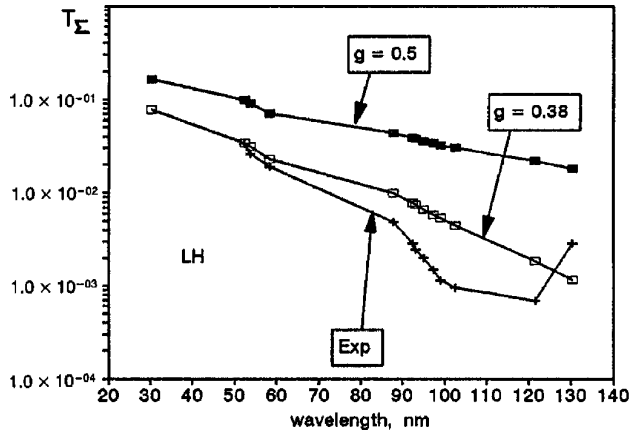

Fig. 4 Spectral dependence of transmission $T_\Sigma = T_P + T_S$. Exp is the experimentally determined values. Calculated dependencies are shown for two different geometrical transparencies, $g = 0.5$ and $g = 0.38$, of the transmission grating. The LH set of gold optical constants was used in these calculations.

With the wavelength decrease all curves are approaching the geometrical transparency of the grating.

The ratio of transmissions, $T_R = T_P/T_S$, is a convenient parameter for describing grating polarization properties. Ratio T_R was experimentally determined at the $\lambda = 58.4$-nm wavelength (Fig. 5), which required measurement of the transmission of two crossed gratings. The measured grating transmission T_S is approximately a factor of 100 smaller than the value of T_P at this wavelength: $T_S = 1.90 \times 10^{-4}$ and $T_P = 1.88 \times 10^{-2}$. The attenuation of unpolarized light (58.4 nm) would be $\sim 10^{-2}$ and 4×10^{-6} by a single grating and crossed grating filters, respectively. The large value of T_R (≈ 100) demonstrates that transmission gratings would serve as efficient polarizers. For example, unpolarized incident radiation at a 58.4-nm wavelength will be highly polarized ($P_T \approx 0.98$) after the grating. The experimental value of T_R (Fig. 5) is more than a factor 10 higher than the theory prediction for nominal grating geometrical characteristics.

During the final measurements of crossed-grating transmission, the gratings were inadvertently damaged. There is a chance that the measurement of T_X (and the derived value of T_S) is partially affected by this accident. However, the effect seems to be small because postaccident measurements did not show significant changes in the single-grating transmissions. The results of crossed-grating measurements should be taken with some caution, and their validity will be verified in the future. Measurements of T_Σ are not affected at all.

The discrepancies between the computed grating filtering characteristics and measurement results (Figs. 4 and 5) have suggested the possible deviation of grating geometrical characteristics from those provided by the manufacturer. The measurment of grating geometrical characteristics is a nontrivial task; for example, a scanning electron microscope can show the structure of the grating surface but cannot reveal possible slit-width variations inside the transmission grating.

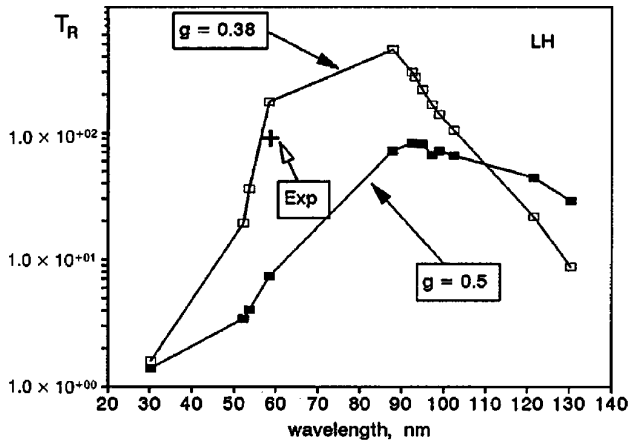

Fig. 5. Spectral dependence of the transmission ratio, $T_R = T_P/T_s$. Exp is the experimentally determined value at the 58.4-nm wavelength. Calculated dependencies are shown for two different geometrical transparencies, $g = 0.5$ and $g = 0.38$, of the transmission grating. The LH set of gold optical constants was used in these calculations.

The computed grating transmission is less dependent on the accuracy of the theoretical model and uncertainty in gold constants at shorter wavelengths. (The transmission approaches the geometrical transparency at $\lambda \ll p$. The grating thickness (455 nm in our case) and period (200 nm) are fixed by fabrication technology[22]; grating geometrical transparency (or efficient geometrical transparency) g is more difficult to control, and it may vary (i.e., gap width d may vary). Therefore one can assume that grating period p and thickness h are known. By varying the geometrical transparency g, one can fit the model predictions with the experimentally observed grating transmission T_Σ at the shortest wavelength where measurements are available ($\lambda = 52.2$ nm in our case). The geometrical transparency, $g = 0.38$, provided the best fit. Note that the geometrical transparency of another grating that was determined by ion-beam attenuation[16] also produced geometrical transparency values smaller than those provided by the manufacturer.

Computer simulations of spectral dependencies, $T_\Sigma(\lambda)$ and $T_R(\lambda)$, for $g = 0.5$ and $g = 0.38$ are compared in Figs. 4 and 5 for the LH gold set. One can see that grating characteristics depend strongly on parameter g. The assumption of the smaller geometrical transparency, $g = 0.38$, results in a significantly better agreement of the calculated transmission, $T_\Sigma(\lambda)$, with the experimental data, although some differences in the spectral dependence remain. The agreement of predicted transmission ratio T_R with the experimentally obtained value is excellent (Fig. 5) at the 58.4-nm wavelength. The definitive verification of the computer code requires measurements of T_P and T_S at larger numbers of wavelengths as well as measurements of light-intensity distribution across nonzero diffraction orders. Large values of transmission ratio T_R require that even the synchrotron light sources, which provide highly polarized radiation and look attractive for future grating studies, should be considered as partially polarized because of the finite angles of acceptance into the monochromator system.[23]

If one assumes that the ratio of transmissions T_R is very large (see Fig. 5), the polarization of the light produced by the monochromator [see Eq. (5)] can be related to measured values R_X and R_Y in the following way:

$$P_0(\lambda) = [R_X(\lambda) - R_Y(\lambda)]/[T_P(\lambda) - T_S(\lambda)] \approx [R_X(\lambda) - R_Y(\lambda)]/[R_X(\lambda) + R_Y(\lambda)]. \quad (9)$$

The light polarization (produced by our Seya–Namioka monochromator), determined according to Eq. (8), is the highest at 58.4 nm ($P = 0.8$), and, with the wavelength increase, the polarization decreases to $P = 0.2$ at 121.6 nm.

To conclude, the measurement results showed that transmission gratings serve as efficient filters and polarizers in the EUV/UV range. Transmission-grating filters can use both crossed-grating configurations and stand-alone single gratings. A crossed-grating filter would limit the field of view of the ENA instruments. ENA cameras with a wide field of view in one dimension can be built on the basis of single-transmission-grating filters. The application of transmission-grating-based filters significantly improves the performance of space instruments for planetary magnetosphere and heliosphere ENA imaging and will provide enhanced capabilities for EUV/UV instruments.

This research is supported by NASA grant NAGW-3520. I thank Mark Schattenburg, who kindly provided transmission gratings for this research, and Erik Anderson for his computer code. I enjoyed useful discussions with Darrell Judge, Howard Ogawa, Lev Pitaevskii, and Earl Scime. The help of Don McMullin with measurements is greatly appreciated.

References

1. M. A. Gruntman, "Submicron structures: promising filters in EUV—a review," in *EUV, X-Ray, and Gamma-Ray Instrumentation for Astronomy,* O. H. Siegmund and R. E. Rothschild, eds., Proc. Soc. Photo-Opt. Instrum. Eng. **1549,** 385–394 (1991).
2. K. C. Hsieh, C. C. Curtis, C. Y. Fan, and M. A. Gruntman, "Techniques for remote sensing of space plasma in the heliosphere via energetic neutral atoms: a review," in *Solar Wind Seven,* E. Marsch and R. Schwenn, eds. (Pergamon, New York, 1991), pp. 357–364.
3. D. J. Williams, E. C. Roelof, and D. G. Mitchell, "Global magnetosphere imaging," Rev. Geophys. **30,** 183–208 (1992).
4. R. W. McEntire and D. G. Mitchell, "Instrumentation for global magnetosphere imaging via energetic neutral atoms," in *Solar System Plasma Physics,* J. H. Waite Jr., J. L. Burch, and R. L. Moore, eds. (American Geophysical Union, Washington, D. C., 1989), pp. 69–80.
5. S. Chakrabarti, F Paresce, S. Bowyer, R. Kimble, and S. Kumar, "The extreme ultraviolet day airglow," J. Geophys. Res. **88,** 4898–4904 (1983).
6. M. A. Gruntman and V. B. Leonas, "Neutral solar wind: possibilities of experimental investigation," Report (Preprint) 825 [Space Research Institute (IKI), Academy of Sciences, Moscow, 1983].
7. A. V. Mitrofanov, "Structurally nonuniform filters for the vacuum ultraviolet and ultrasoft x-ray regions of the spectrum," Instrum. Exp. Tech. USSR **26,** 971–974 (1983).
8. G. N. Flerov and V. S. Barashenkov, "Practical applications of heavy ion beams," Sov. Phys. Usp. **17,** 783–793 (1975).
9. B. E. Fischer and R. Spohr, "Production and use of nuclear tracks: imprinting structure on solids," Rev. Mod. Phys. **55,** 907–948 (1983).
10. R. Spohr, *Ion Tracks and Microtechnology* (Friedriech Vieweg & Sons, Braunschweig, 1990).
11. A. V. Mitrofanov and P. Y. Apel, "Porous plastic membranes used as extreme and far ultraviolet radiation diffraction filters," Nucl. Instrum. Methods Phys. Res. A **282,** 542–545 (1989).
12. M. L. Schattenburg, E. H. Anderson, and H. I. Smith, "X-ray/VUV transmission gratings for astrophysical and laboratory applications," Phys. Scr. **41,** 13–20 (1990).
13. J. M. Carter, D. B. Olster, M. L. Schattenburg, A. Yen, and H. J. Smith, "Large-area, free-standing gratings for atom interferometry produced using holographic lithography," J. Vac. Sci. Technol. B **10,** 2909–2911 (1992).
14. H. S. Ogawa, D. R. McMullin, D. L. Judge, and R. Korde, "Normal incidence spectrophotometer with high density transmission grating technology and high-efficiency silicon photodiodes for absolute solar extreme-ultraviolet irradiance measurements," Opt. Eng. **32,** 3121–3125 (1993).
15. E. E. Scime, H. O. Funsten, D. J. McComas, and K. R. Moore, "Low energy neutral atom imaging of the Earth's magnetosphere," Eos Trans. AGU Spring Meeting Suppl. **75**(16), 258 (1994).
16. E. E. Scime, E. H. Anderson, D. J. McComas, and M. L. Schattenburg, "Extreme ultraviolet polarization and filtering with gold transmission gratings," Appl. Opt. **34,** 648–654 (1995).
17. M. A. Gruntman, D. R. McMullin, and D. L. Judge, "Diffraction filtering of EUV radiation for ENA imaging applications," Eos Trans. AGU Spring Meeting Suppl. **75**(16), 259 (1994).
18. J. Tomc, P. Zetner, W. R. Westerveld, and J. W. McConckey, "Variations in the polarization sensitivity of microchannel plates with photon incidence angle and wavelength in the VUV," Appl. Opt. **23,** 656–657 (1984).
19. E. H. Anderson,. "Fabrication and electromagnetic applications of periodic nanostructures," Ph.D. dissertation (Massachusetts Institute of Technology, Cambridge, Mass., 1988).
20. J. H. Weaver, C. Krafka, D. W. Lynch, and E. E. Koch, *Optical Properties of Metals* (Fachinformationszentrum Energie, Physik, Mathematik GmbH, Karlsruhe, 1981), Pt. 2, Nr. 18-2.
21. D. W. Lynch and W. R. Hunter, "Comments on the optical constants of metals and an introduction to the data for several metals," in *Handbook of Optical Constants of Solids* E. D. Palik, ed. (Academic, New York, 1985), pp. 275–295.
22. M. Schattenberg, Center for Space Research, Massachusetts Institute of Technology, Cambridge, Mass. 02139-4307 (personal communication, 1994).
23. J. A. R. Samson, "Polarized vacuum ultraviolet and X-radiation," Nucl. Instrum. Methods **152** 225–230 (1978).